Bulk Synthesis of Large Diameter Semiconducting Single-Walled Carbon Nanotubes by Oxygen-Assisted Floating Catalyst Chemical Vapor Deposition

ARTICLE *in* JOURNAL OF THE AMERICAN CHEMICAL SOCIETY · MARCH 2011

Impact Factor: 12.11 · DOI: 10.1021/ja2008278 · Source: PubMed

9 AUTHORS, INCLUDING:

Ying Tian
Aalto University
33 PUBLICATIONS **877** CITATIONS
SEE PROFILE

Shisheng Li
National University of Singapore
16 PUBLICATIONS **505** CITATIONS
SEE PROFILE

Feng Li
Chinese Academy of Sciences
212 PUBLICATIONS **13,850** CITATIONS
SEE PROFILE

Hui-Ming Cheng
Shenyang National Laboratory for Materials …
486 PUBLICATIONS **33,297** CITATIONS
SEE PROFILE

JACS
JOURNAL OF THE AMERICAN CHEMICAL SOCIETY

COMMUNICATION

pubs.acs.org/JACS

Bulk Synthesis of Large Diameter Semiconducting Single-Walled Carbon Nanotubes by Oxygen-Assisted Floating Catalyst Chemical Vapor Deposition

Bing Yu,[†,§] Chang Liu,[†,§] Peng-Xiang Hou,[†] Ying Tian,[‡] Shisheng Li,[†] Bilu Liu,[†] Feng Li,[†] Esko I. Kauppinen,[‡] and Hui-Ming Cheng*[,†]

[†]Shenyang National Laboratory for Materials Science, Institute of Metal Research, Chinese Academy of Sciences, Shenyang 110016, People's Republic of China

[‡]NanoMaterials Group, Department of Applied Physics and Center for New Materials, School of Science, Aalto University, P.O. Box 15100, FI-00076 Aalto, Finland

Supporting Information

ABSTRACT: Semiconducting single-walled carbon nanotubes (s-SWCNTs) with a mean diameter of 1.6 nm were synthesized on a large scale by using oxygen-assisted floating catalyst chemical vapor deposition. The oxygen introduced can selectively etch metallic SWCNTs *in situ*, while the sulfur growth promoter functions in promoting the growth of SWCNTs with a large diameter. The electronic properties of the SWCNTs were characterized by laser Raman spectroscopy, absorption spectroscopy, and field effect transistor measurements. It was found that the content of s-SWCNTs in the samples was highly sensitive to the amount of oxygen introduced. Under optimum synthesis conditions, enriched s-SWCNTs can be obtained in milligram quantities per batch.

Single-walled carbon nanotube (SWCNT)-based high-performance electronic devices are one of the most appealing applications of carbon nanotubes (CNTs).[1] It is highly important and challenging to selectively prepare semiconducting SWCNTs (s-SWCNTs), since SWCNTs synthesized by conventional methods are usually a mixture of s-SWCNTs and metallic SWCNTs (m-SWCNTs).[2] Considerable research effort has been dedicated to preparing s-SWCNTs by *in situ* ultraviolet radiation,[3] tuning of the carbon source[4] and growth temperature,[5] plasma enhancement,[6] optimization of the composition and pretreatment of catalysts,[7] and postsynthesis treatments.[8] The drawback of the post-treatment methods is that contamination and defects are inevitably introduced. On the other hand, the reported direct synthesis of s-SWCNTs is usually realized by surface growth, yielding a very limited amount of sample. In addition, the performance of SWCNT-based field effect transistors (FETs) depends greatly on the diameter of the SWCNTs,[7c,9] and an appropriate and narrow diameter distribution of s-SWCNTs is critical to achieve the desired performance and uniformity of the devices fabricated. Although the preparation of specific (n, m) enriched SWCNTs has been reported, the coexistence of m-SWCNTs cannot be excluded. And the diameters of these SWCNTs are usually smaller than 1.0 nm, which is considered too small for assembling electronic devices.[7c,9] Here we report a selective synthesis of s-SWNTs with a narrow and suitable diameter distribution in milligram quantities by oxygen-assisted floating catalyst chemical vapor deposition (FCCVD), where oxygen is used to selectively etch m-SWCNTs *in situ*, and the sulfur growth promoter functions to enhance the growth of SWCNTs and tune their diameter. Under optimized conditions, samples containing ~90% s-SWCNTs with diameters largely in the range 1.4−1.8 nm were obtained.

The details of the synthesis procedure are described in Supporting Information (SI) 1.1. Briefly, ferrocene and sulfur, which serve as a catalyst precursor and growth promoter, respectively, were pressed into a tablet and placed upstream of a quartz tube reactor inserted into a tubular furnace. The vaporized ferrocene and sulfur were carried into the reaction zone by mixed H_2 (carrier gas), CH_4 (carbon source), and O_2 (oxidant) for the growth of the SWCNTs. SWCNT thin films were collected at downstream of the reactor or from the filter connected to the tail gas pipe. The as-prepared SWCNTs were purified by heat treatment in air at 200 °C for 2−5 h and a following hydrochloric acid immersion (see SI 1.2 for details). The structure and electronic properties of the purified SWCNTs were characterized using transmission electron microscopy (TEM), laser Raman spectroscopy, absorption spectroscopy, and FET measurements.

Figure 1a and b are representative TEM images of the SWCNTs prepared by the oxygen-assisted FCCVD. It can be seen that the SWCNTs are rather straight and there is almost no amorphous carbon attached to the tube surface. Diameters of ~160 SWCNTs were measured by TEM, and the resultant histogram of the diameter distribution is plotted in Figure 1c. The diameters are largely centered in the range 1.4−1.8 nm. A mean diameter of 1.6 nm was obtained, much larger than those of HiPCO and CoMoCAT SWCNTs. The larger diameter of the SWCNTs can be attributed to the addition of the sulfur growth promoter, which functions by facilitating the localized nucleation of SWCNTs and yielding CNTs with large diameters.[10] It has been reported that the optimum diameter distribution of s-SWCNTs for fabricating FETs is 1.6−2.0 nm, because such CNTs can provide band gaps that lead to high on/off ratios and good electrical contacts owing to the low tunneling barriers

Received: January 27, 2011
Published: March 16, 2011

dx.doi.org/10.1021/ja2008278 | J. Am. Chem. Soc. 2011, 133, 5232–5235

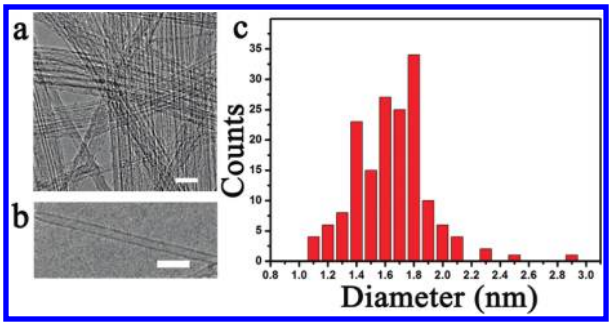

Figure 1. (a and b) Typical TEM images of the SWCNTs prepared by the FCCVD, showing their high quality; scale bar: 10 nm. (c) A histogram showing the diameter distribution of the SWCNTs.

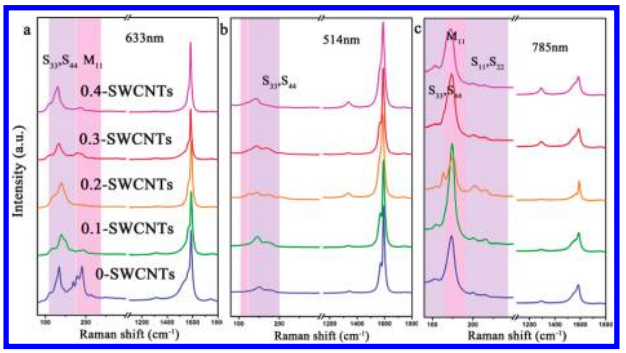

Figure 2. (a, b, and c) Raman spectra of the 0- (blue), 0.1- (green), 0.2- (orange), 0.3- (red), and 0.4- (pink) SWCNT samples excited with laser wavelengths of 633, 514, and 785 nm, respectively. The regions corresponding to semiconducting transitions are labeled as $S_{11,22}$ and $S_{33,44}$ (shaded blue), and the first-order metallic transition is labeled as M_{11} (shaded pink). The Raman spectra were normalized according to the G-band intensity.

and Schottky barriers.[7c,9] Therefore, these SWCNTs with a larger diameter may be more applicable for assembling electronic devices.

Our previous work showed that the existence of a small amount of oxygen can introduce structural defects in m-SWCNTs synthesized by FCCVD.[8f] Hydroxyl radicals might be formed preferentially on the side wall of m-SWCNTs because of their relative smaller ionization potential.[7] Therefore, it would be possible to completely remove m-SWCNTs and produce pure s-SWCNTs on a large scale by using this oxygen-assisted FCCVD, if suitable *in situ* oxidation conditions could be found. Therefore, we studied the effect of the oxygen flow rate on the structure and properties of SWCNTs. With a H_2 flow of 500 sccm, CH_4 flow of 3 sccm, and growth temperature of 1100 °C maintained, oxygen flows of 0, 0.1, 0.2, 0.3, and 0.4 sccm were explored for the growth of SWCNTs. The SWCNT samples thus obtained are denoted as 0-SWCNT, 0.1-SWCNT, 0.2-SWCNT, 0.3-SWCNT, and 0.4-SWCNT hereafter.

These samples were examined by laser Raman spectroscopy with excitation wavelengths of 633, 514, and 785 nm. Figure 2a−c present the Raman spectra of the five samples, where the RBM peaks originating from m- and s-SWCNTs are highlighted according to the Kataura plot.[11] In Figure 2a, we can see that the RBM peak intensities of m- and s-SWCNTs, located at ∼110 and 240 cm^{-1}, are similar for the 0-SWCNT sample. And the highest RBM peak intensity ratio of s-/m-SWCNTs is achieved for the 0.2-SWCNT sample, in which the signal of m-SWCNTs becomes almost undetectable. In Figure 2b, the RBM peaks originating from

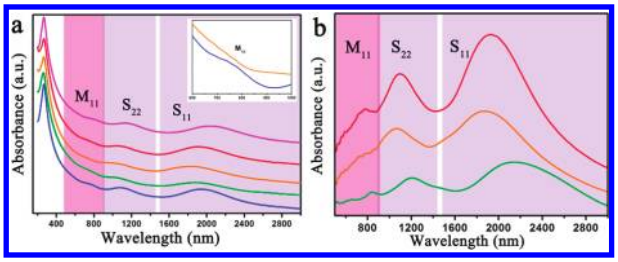

Figure 3. (a) Absorption spectra of the 0- (blue), 0.1- (green), 0.2- (orange), 0.3- (red), and 0.4- (pink) SWCNT samples, and the inset shows enlarged absorption spectra of the 0- and 0.2-SWCNTs. The labels S_{11} and S_{22} (shaded blue) indicate the excitonic optical absorption bands of s-SWCNTs, and the M_{11} label (shaded pink) corresponds to the first-order transition of m-SWCNTs. The spectra were offset for clarity, but the intensity scale is the same for all spectra. (b) Absorption spectra of the 0.1-, 0.2-, and 0.3-SWCNT samples with background subtracted.

m-SWCNTs were scarcely observed when an excitation wavelength of 514 nm was used. According to the Kataura plot, only s-SWCNTs with diameters of 1.4−1.8 nm can be excited by the 514 nm laser. Figure 2c shows the Raman spectra of the samples excited by the 785 nm laser. A comparison on the RBM peak intensities of the samples reveals that the highest s-/m-SWCNT ratio is again achieved for the 0.2-SWCNT sample. And the G-band of the 0.2-SWCNTs shows a Lorentzian line shape, which is characteristic of s-SWCNTs and is quite different from those of other samples. These results indicate that effective enrichment of s-SWCNTs is realized for the 0.2-SWCNT sample.[7b] During the oxygen-assisted FCCVD growth of SWCNTs, the slightly different antioxidation capabilities of m- and s-SWCNTs allow m-SWCNTs to be preferentially etched and removed by the *in situ* oxidation due to their smaller ionization potential.[12] Too active oxidation conditions will lead to simultaneous loss of s- and m-SWCNTs and hence decrease the enrichment efficiency. In this work, an optimum oxygen flow rate of 0.2 sccm (∼0.04% of the total gas flow) is determined for the selective synthesis of s-SWCNTs. We note that, although the content of s-SWCNTs is effectively improved, the m-SWCNT signal was still detected for the 0.2-SWCNT sample with an excitation laser wavelength of 785 nm, as shown in Figure 2c. This is because some m-SWCNTs with large diameters may remain after the *in situ* oxidation process. However, the amount of such m-SWCNTs is very small, since the Lorentzian line shape indicates that the majority of the 0.2-SWCNT sample is semiconducting.

To further confirm the enrichment of s-SWCNTs in the 0.2-SWCNT sample, the optical absorption spectra of the five samples were measured, and the typical UV−vis−NIR spectra obtained are shown in Figure 3. The spectroscopic characterization was performed using the SWCNT thin films collected from a preset filter (for details see SI 1.3 and 1.4). As shown in Figure 3a, the peaks located at 500−900 nm, corresponding to the first van Hove singularity transition of m-SWCNTs (M_{11}),[13] disappeared for the 0.2-SWCNT sample. This change is more clearly evident in the inset, where enlarged spectra of 0- and 0.2-SWCNTs are shown. This result suggests that the 0.2-SWCNT sample is s-SWCNT dominant, coinciding well with the Raman characterization. The broad absorption bands in the spectra originate from the small SWCNT bundles existing in the SWCNT thin films. To estimate the relative weight ratio of metallic-to-semiconducting nanotubes in the SWCNT samples, the background was first subtracted based on the nonlinear model[14] and the resulting spectra are plotted in Figure 3b. The weight ratios (r) of metallic tubes (W_M) and

dx.doi.org/10.1021/ja2008278 |*J. Am. Chem. Soc.* 2011, 133, 5232–5235

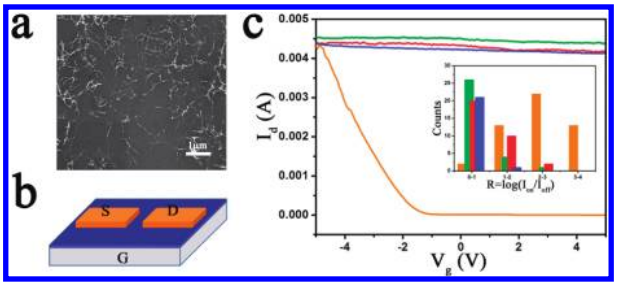

Figure 4. (a) A representative SEM image of the SWCNT thin film. (b) Diagram showing the configuration of a TFT (S = source; G = gate; D = drain). The SWCNT networks were formed on a silicon wafer with a 100-nm thick SiO_2 layer thermally grown on the surface, which serves as a gate dielectric. (c) Typical transport characteristics of the 0- (blue), 0.1- (green), 0.2- (orange), and 0.3- (red) SWCNT-based TFTs: drain current I_d vs top gate voltage V_g, the bias voltage V_{ds} was maintained at 100 mV. The inset shows the statistical result of I_{on}/I_{off} for the SWCNT-based TFTs.

semiconducting tubes (W_S) were estimated from the corresponding absorption peak areas using the formula $r = W_M/(W_S + W_M)$, and the detailed calculations are described in SI 2. The smallest r value of 0.12 was achieved for the 0.2-SWCNT sample, which is much lower than that of the 0-SWCNT sample (~0.30), indicating that m-SWCNTs have been effectively removed by introducing an appropriate amount of oxygen. And the content of s-SWCNTs in the 0.2-SWCNT sample is estimated to be around 90%.[15]

Electrical measurements can provide direct evidence of the transport properties of SWCNTs.[1a,16] Thus, thin-film field effect transistor (TFT) devices based on the SWCNTs were fabricated (more details are presented in SI 1.5). Figure 4a shows a typical SEM image of the SWCNT thin film used. It can be seen that an SWCNT network is formed, and the thickness of the thin film is about 50 nm. Figure 4b is a diagram showing the structure of an SWCNT-based TFT. The width of the source and drain electrodes is 5 μm, and the channel between the source and drain is 2 μm in width. The gate leakage current associated with the gate bias is of the order of picoamperes and is therefore negligible. Four TFTs based on the 0-, 0.1-, 0.2- and 0.3-SWCNT samples were constructed and measured under identical conditions. Figure 4c presents the typical transfer characteristics of the TFTs. For the 0-, 0.1-, and 0.3-SWCNT samples, the devices show on/off ratios of less than 10 due to the coexistence of s- and m-SWCNTs. However, a much higher on/off ratio of 10^4 was achieved for the 0.2-SWCNT sample, indicating a high content of s-SWCNTs. The inset of Figure 4c shows a statistical plot of the I_{on}/I_{off} ratios from 50 TFTs based on the 0.2-SWCNTs and 30 TFTs based on the 0-, 0.1-, and 0.3-SWCNTs. It can be seen that the I_{on}/I_{off} of the 0.2-SWCNTs is clearly larger than those of the other samples. More than 70% of the 0.2-SWCNT-based TFTs show I_{on}/I_{off} values larger than 100, and more than 96% have values greater than 10. These statistics confirm that the selective synthesis of s-SWCNTs has been realized by the oxygen-assisted FCCVD.

We also propose a mechanism accounting for the selective growth of s-SWCNTs by this method as follows: m-SWCNTs are considered to be more reactive than semiconducting ones due to their smaller ionization potential.[4,12] The slightly different antioxidation capability between m- and s-SWCNTs makes it possible that m-SWCNTs be preferentially etched and removed by the *in situ* oxidation. And it is critical to find out the appropriate oxidation conditions that allow removal of m-SWCNTs while keeping s-SWCNTs intact. In this study, when a suitable amount of oxygen was introduced (0.2 sccm), samples containing a high percentage of s-SWCNTs were obtained. It is worth noting that the diameter of SWCNTs may also influence their antioxidation capability due to their different curvatures,[17] and SWCNTs with larger diameters are generally more stable. Actually, a few large diameter m-SWCNTs remaining after the oxidation are detectable by the multiwavelength laser Raman characterization (Figure 2). Therefore, to further improve the selective growth efficiency of s-SWCNTs by the *in situ* oxidation approach, it is important to have their diameters well controlled in a narrower range.

In summary, we realized the selective synthesis of large diameter s-SWCNTs on a large scale using an oxygen-assisted FCCVD. TEM observations reveal that the diameters of the SWCNTs are largely located in the range 1.4−1.8 nm, and the relative larger diameter can be attributed to the tuning effect of a sulfur growth promoter. Combined laser Raman spectroscopy, absorption spectroscopy, and TFT characteristic measurements show that an s-SWCNT dominant sample can be obtained when a suitable amount of oxygen is used, which functions in preferentially etching m-SWCNTs during the synthesis process. These s-SWCNTs with a mean diameter of 1.6 nm will be promising for electronic device (such as FET) fabrication. The bulk synthesis allows necessary pretreatment and processing of the SWCNTs prior to/during the assembly of the devices.

■ ASSOCIATED CONTENT

Supporting Information. Synthesis details, purification process, absorption spectroscopy measurement, fabrication of FETs, and background subtraction of absorption spectra. These materials are available free of charge via the Internet at http://pubs.acs.org.

■ AUTHOR INFORMATION

Corresponding Author
cheng@imr.ac.cn

Author Contributions
§These authors contributed equally.

■ ACKNOWLEDGMENT

We thank Ms. Xi Ling for help in 514 and 785 nm Raman measurements. The authors also thank Prof. Xiaojun Tian for the supply of Au electrodes. We acknowledge financial support from MOST of China (Grants 2011CB932601, 2011CB932604, and 2008DFA51400), NSFC (Grants 50921004 and 50872137), Aalto University through the Multidisciplinary Institute of Digitalization and Energy (MIDE) program via a CNB-E project, and TEKES, Finland.

■ REFERENCES

(1) (a) Tans, S. J.; Verschueren, A. R. M.; Dekker, C. *Nature* **1998**, *393*, 49. (b) Yao, Z.; Kane, C. L.; Dekker, C. *Phys. Rev. Lett.* **2000**, *84*, 2941. (c) Javey, A.; Kim, H.; Brink, M.; Wang, Q.; Ural, A.; Guo, J.; McIntyre, P.; McEuen, P.; Lundstrom, M.; Dai, H. J. *Nat. Mater.* **2002**, *1*, 241.

(2) (a) Saito, R.; Fujita, M.; Dresselhaus, G.; Dresselhaus, M. S. *Appl. Phys. Lett.* **1992**, *60*, 2204. (b) Avouris, P. *Acc. Chem. Res.* **2002**, *35*, 1026.

(3) Hong, G.; Zhang, B.; Peng, B.; Zhang, J.; Choi, W.; Choi, J.; Kim, J.; Liu, Z. *J. Am. Chem. Soc.* **2009**, *131*, 14642.

(4) Ding, L.; Tselev, A.; Wang, J. Y.; Yuan, D. N.; Chu, H. B.; McNicholas, T. P.; Li, Y.; Liu, J. *Nano Lett.* **2009**, *9*, 800.

(5) (a) Loebick, C. Z.; Podila, R.; Reppert, J.; Chudow, J.; Ren, F.; Haller, G. L.; Rao, A. M.; Pfefferle, L. D. *J. Am. Chem. Soc.* **2010**, *132*, 11125. (b) Ghorannevis, Z.; Kato, T.; Kaneko, T.; Hatakeyama, R. *J. Am. Chem. Soc.* **2010**, *132*, 9570.

(6) Qu, L. T.; Du, F.; Dai, L. M. *Nano Lett.* **2008**, *8*, 2682.

(7) (a) Chiang, W. H.; Sankaran, R. M. *Nat. Mater.* **2009**, *8*, 882. (b) Harutyunyan, A. R.; Chen, G. G.; Paronyan, T. M.; Pigos, E. M.; Kuznetsov, O. A.; Hewaparakrama, K.; Kim, S. M.; Zakharov, D.; Stach, E. A.; Sumanasekera, G. U. *Science* **2009**, *326*, 116. (c) Wang, H.; Wang, B.; Quek, X. Y.; Wei, L.; Zhao, J. W.; Li, L. J.; Chan-Park, M. B.; Yang, Y. H.; Chen, Y. A. *J. Am. Chem. Soc.* **2010**, *132*, 16747. (d) He, M.; Chernov, A. I.; Fedotov, P. V.; Obraztsova, E. D.; Sainio, J.; Rikkinen, E.; Jiang, H.; Zhu, Z.; Tian, Y.; Kauppinen, E. I.; Niemela, M.; Krauset, A. O. I. *J. Am. Chem. Soc.* **2010**, *132*, 13994.

(8) (a) Zheng, M.; Jagota, A.; Strano, M. S.; Santos, A. P.; Barone, P.; Chou, S. G.; Diner, B. A.; Dresselhaus, M. S.; McLean, R. S.; Onoa, G. B.; Samsonidze, G. G.; Semke, E. D.; Usrey, M.; Walls, D. J. *Science* **2003**, *302*, 1545. (b) Zhang, G. Y.; Qi, P. F.; Wang, X. R.; Lu, Y. R.; Li, X. L.; Tu, R.; Bangsaruntip, S.; Mann, D.; Zhang, L.; Dai, H. J. *Science* **2006**, *314*, 974. (c) Arnold, M. S.; Green, A. A.; Hulvat, J. F.; Stupp, S. I.; Hersam, M. C. *Nat. Nanotechnol.* **2006**, *1*, 60. (d) Voggu, R.; Rao, K. V.; George, S. J.; Rao, C. N. R. *J. Am. Chem. Soc.* **2010**, *132*, 5560. (e) Tanaka, T.; Jin, H.; Miyata, Y.; Fujii, S.; Suga, H.; Naitoh, Y.; Minari, T.; Miyadera, T.; Tsukagoshi, K.; Kataura, H. *Nano Lett.* **2009**, *9*, 1497. (f) Yu, B.; Hou, P. X.; Li, F.; Liu, B. L.; Liu, C.; Cheng, H. M. *Carbon* **2010**, *48*, 2941.

(9) (a) Kim, W.; Javey, A.; Tu, R.; Cao, J.; Wang, Q.; Dai, H. J. *Appl. Phys. Lett.* **2005**, *87*, 173101. (b) Durrer, L.; Greenwald, J.; Helbling, T.; Muoth, M.; Riek, R.; Hierold, C. *Nanotechnology* **2009**, *20*, 355601.

(10) Ren, W. C.; Li, F.; Bai, S.; Cheng, H. M. *J. Nanosci. Nanotechnol.* **2006**, *6*, 1339.

(11) Strano, M. S. *J. Am. Chem. Soc.* **2003**, *125*, 16148.

(12) Lu, J.; Nagase, S.; Zhang, X. W.; Wang, D.; Ni, M.; Maeda, Y.; Wakahara, T.; Nakahodo, T.; Tsuchiya, T.; Akasaka, T.; Gao, Z. X.; Yu, D. P.; Ye, H. Q.; Mei, W. N.; Zhou, Y. S. *J. Am. Chem. Soc.* **2006**, *128*, 5114.

(13) Strano, M. S.; Dyke, C. A.; Usrey, M. L.; Barone, P. W.; Allen, M. J.; Shan, H. W.; Kittrell, C.; Hauge, R. H.; Tour, J. M.; Smalley, R. E. *Science* **2003**, *301*, 1519.

(14) (a) Nair, N.; Usrey, M. L.; Kim, W. J.; Braatz, R. D.; Strano, M. S. *Anal. Chem.* **2006**, *78*, 7689. (b) Tian, Y.; Jiang, H.; von Pfaler, J.; Zhu, Z.; Nasibulin, A. G.; Nikitin, T.; Aitchison, B.; Khriachtchev, L.; Brown, D. P.; Kauppinen, E. I. *J. Phys. Chem. Lett.* **2010**, *1*, 1143. (c) Ryabenko, A. G.; Dorofeeva, T. V.; Zvereva, G. I. *Carbon* **2004**, *42*, 1523.

(15) (a) Itkis, M. E.; Perea, D. E.; Niyogi, S.; Rickard, S. M.; Hamon, M. A.; Zhao, B.; Haddon, R. C. *Nano Lett.* **2003**, *3*, 309. (b) Miyata, Y.; Yanagi, K.; Maniwa, Y.; Kataura, H. *J. Phys. Chem. C* **2008**, *112*, 13187.

(16) Martel, R.; Schmidt, T.; Shea, H. R.; Hertel, T.; Avouris, P. *Appl. Phys. Lett.* **1998**, *73*, 2447.

(17) Zhou, W.; Ooi, Y. H.; Russo, R.; Papanek, P.; Luzzi, D. E.; Fischer, J. E.; Bronikowski, M. J.; Willis, P. A.; Smalley, R. E. *Chem. Phys. Lett.* **2001**, *350*, 6.